Functionalized Basket-Shaped Hosts. Synthesis and Complexation Studies with (Alkali) Metal and Ammonium and Diammonium Ions

Jan W. H. Smeets,† Lydia van Dalen,† Veronica E. M. Kaats-Richter,† and Roeland J. M. Nolte*,‡

Department of Organic Chemistry, University of Utrecht, 3584 CH Utrecht, The Netherlands, and Department of Organic Chemistry, University of Nijmegen, 6525 ED Nijmegen, The Netherlands

Received July 26, 1989

Functionalized basket-shaped hosts have been synthesized from the concave building block 1,3:4,6-bis(3,6-dihydroxy-1,2-xylylene)tetrahydro-3a,6a-diphenylimidazo[4,5-*d*]imidazole-2,5(1*H*,3*H*)-dione (**1**). To this end, N-substituted 1,4,10,13-tetraoxa-7-azatridecamethylene bridges were attached to the 3,6- and 3′,6′-positions of the xylylene rings of **1**. The substituents at the nitrogen atom in the bridge include: 5-hydroxy-3-oxapentyl, benzyl, hydrogen, 5-(*N*-(benzyloxycarbonyl)-L-histidyl)-3-dioxapentyl, and 5-acetyl-3-oxapentyl. The baskets complex alkali metal and ammonium guests, as well as aliphatic and aromatic diammonium guests, all in a 1:1 ratio. Using the picrate extraction technique, free energies of binding for the new hosts with 19 guests were determined. Extremely strong binding ($-\Delta G°$ values up to 18 kcal mol^{-1}) was observed for the complexes between the hosts and *o*-phenylenediammonium dipicrate. The origin of this phenomenon is discussed. The host with histidyl substituents easily forms a 1:1 complex with $Zn(OTf)_2$.

Introduction

Dating from its earliest descriptions by Pedersen, Cram, and Lehn, host–guest or supramolecular chemistry has become a rapidly growing field.[1] Within this field current research is aimed at the development of artificial systems that mimic enzymatic catalysis, regulation, and transport. Our particular interest is in the construction of host–guest systems that show catalytic properties.[1m,n] For this purpose, we have undertaken the synthesis of host molecules that possess a cavity or cleft with binding sites for substrates and a catalytic center in the immediate environment of this cavity. In enzymes, such a center very often contains a metal atom. For example, there are no less than 20 zinc-containing metallo-enzymes known, of which carbonic anhydrase and carboxypeptidase are the best studied examples.[2]

Recently, we described a novel concave building block for the construction of organic hosts (**1**) (Figure 1). This building block is a diphenylglycoluril molecule flanked on either side by an *o*-xylylene unit.[3] X-ray analysis and ^{1}H NMR experiments prove that the overall structure of this compound is rigid and concave. Using this building block, a variety of host molecules with interesting binding properties have been constructed.[3a] One type of host belonging to this family is the basket-shaped host (Figure 2). This molecule is able to complex alkali metal salts and aliphatic and aromatic (di)ammonium salts. Depending on the length of the oligooxyethylene handles of the baskets, the stoichiometry of the complexes varies from 1:1 to 1:2 (host:guest).[3b] In this paper we present new basket-shaped molecules which contain an additional side arm at each handle (Figure 3). These side arms are connected via a nitrogen atom that is incorporated into the handle of the basket. The synthesis and binding properties of these baskets are discussed. Additionally, we present a basket whose side arms are equipped with a coordinating imidazole group as part of a histidine molecule. This basket readily complexes a metal atom, e.g. a zinc ion, to form a metallo-host.[1m]

Results and Discussion

Synthesis. The synthetic route which led to the baskets (Chart I) is presented in Scheme I. Building block **1** was prepared from urea, benzil, hydroquinone, and formaldehyde according to a procedure previously published by us.[3] It was equipped with four oxyethylene chains terminated with four chlorine groups, by reaction with a slight excess of 1-tosyl-5-chloro-3-oxapentane and powdered KOH as a base in DMSO, to give **2** in 74% yield. This compound was allowed to react with 5 equiv of the primary amines 2-(2-aminoethoxy)ethanol or benzylamine using potassium carbonate as a base and a catalytic amount of potassium iodide in DMSO. The products of this reaction, compounds **3a** and **3b**, were obtained in yields of 40% and 52%, respectively. It is important that the ratio between the primary amine and **2** be exactly 5. At a lower ratio the conversion of **2** is incomplete; at a higher ratio, ring closure occurs only partially or not at all, as additional molecules of the amine react with **2** to give secondary amines. Hydrogenation of compound **3b** using 10% Pd/C in acetic acid gave **3c** in 70% yield. Compound **3d** was synthesized by reaction of **3a** with 2 equiv of *N*-(benzyloxycarbonyl)-L-histidine according to a standard procedure in DMF at 0 °C (46% yield).[4]

For characterization purposes, we also acetylated compound **3a** using acetic acid anhydride and pyridine to yield **3e**. The ^{1}H NMR spectrum of this derivative shows two peaks for the $CH_3C(O)$ protons, while FAB mass spec-

† University of Utrecht.
‡ Univeristy of Nijmegen.

(1) (a) Cram, D. J. *Science* **1988**, *240*, 760–767. (b) Hosseini, M. W.; Blacker, A. J.; Lehn, J.-M. *J. Chem. Soc., Chem. Commun.* **1988**, 596–598. (c) Albrecht-Gary, A.-M.; Dietrich-Buchecker, C.; Saad, Z.; Sauvage, J.-P. *J. Am. Chem. Soc.* **1988**, *110*, 1467–1472. (d) Wolfe, J.; Nemeth, D.; Costero, A.; Rebek, J. *J. Am. Chem. Soc.* **1988**, *110*, 983–984. (e) Dharanipragada, R.; Ferguson, S. B.; Diederich, F. *J. Am. Chem. Soc.* **1988**, *110*, 1679–1690. (f) Grootenhuis, P. D. J.; van Eerden, J.; Dijkstra, P. J.; Harkema, S.; Reinhoudt, D. N. *J. Am. Chem. Soc.* **1987**, *109*, 8044–8051. (g) O'Krongly, D.; Denmeade, S. R.; Chiang, M. Y.; Breslow, R. *J. Am. Chem. Soc.* **1985**, *107*, 5545–5545. (h) Collet, A. *Tetrahedron* **1987**, *43*, 5725–5759. (i) Delgado, M.; Gustowski, D. A.; Yoo, H. K.; Gatto, V. J.; Gokel, G. W.; Echegoyen, L. *J. Am. Chem. Soc.* **1988**, *110*, 119–124. (j) Mock, W. L.; Shih, N.-Y. *J. Am. Chem. Soc.* **1988**, *101*, 4706–4710. (k) Sutherland, I. O. *Chem. Soc. Rev.* **1986**, 63–91. (l) Vögtle, F. *Tetrahedron* **1987**, *43*, 2065–2074. (m) Niele, F. G. M.; Nolte, R. J. M. *J. Am. Chem. Soc.* **1988**, *110*, 172–177. (n) Niele, F. G. M.; Martens, C. F.; Nolte, R. J. M. *J. Am. Chem. Soc.* **1989**, *111*, 2078–2085. (o) Van Esch, J.; Roks, M. F. M.; Nolte, R. J. M. *J. Am. Chem. Soc.* **1986**, *108*, 6093–6094.

(2) (a) Harsuck, J. A.; Libscomb, W. N. *Enzymes, 3rd ed., 1970–1976* **1970**, *3*, 1. (b) Sundberg, R. J.; Martin, R. B. *Chem. Rev.* **1974**, *74*, 471–517.

(3) (a) Smeets, J. W. H.; Sijbesma, R. P.; Niele, F. G. M.; Spek, A. L.; Smeets, W. J. J.; Nolte, R. J. M. *J. Am. Chem. Soc.* **1987**, *109*, 928–929. (b) Smeets, J. W. H.; Sijbesma, R. P.; van Dalen, L.; Spek, A. L.; Smeets, W. J. J.; Nolte, R. J. M. *J. Org. Chem.* **1989**, *54*, 3710–3717. (c) Smeets, J. W. H.; Visser, H. C.; Kaats-Richters, V. E. M.; Nolte, R. J. M. *Recl. Trav. Chim. Pays-Bas*, in press.

(4) Bodansky, M.; Vigneaud, V. D. *J. Am. Chem. Soc.* **1959**, *81*, 6072.

0022-3263/90/1955-0454$02.50/0

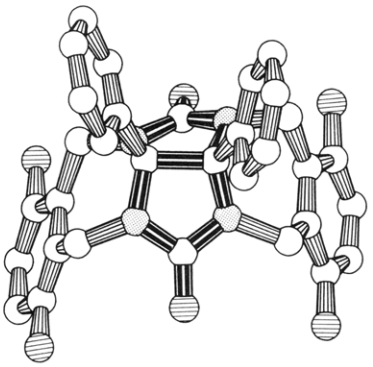

Figure 1. Crystal structure of building block 1. Hydrogen atoms have been omitted for clarity.

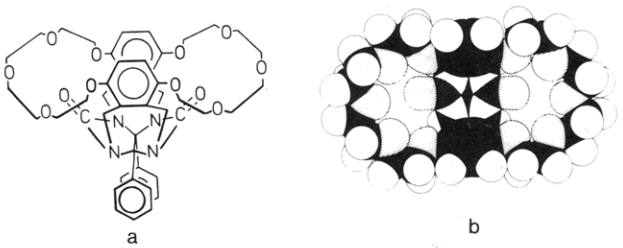

Figure 2. Side-view drawing (a) and CPK model (b) of a basket-shaped host. The receptor sites are formed by the oxygen atoms of the urea units and the oxyethylene bridges.

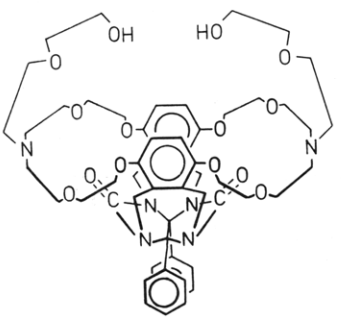

Figure 3. An example of a functionalized basket (**3a**). One side chain is connected to each of the nitrogen atoms of the handles of the baskets.

troscopy gives a large signal for $(M + H + \text{acetic anhydride})^+$, aside from the signal due to $(M + H)^+$. Apparently, acetic anhydride is very strongly complexed in the basket. Even after 1 day under high vacuum the large signal did not disappear.

Reaction of **2** with 2-methoxyethylamine was not successful. In spite of all adjustments to both the ratio of the two components as well as the reaction conditions, only negligible amounts of product were obtained as judged by ^{1}H NMR and FAB mass spectroscopy. The reason for this failure is not clear.

Baskets **3a–e** were characterized by FAB MS, elemental analyses, and infrared and ^{1}H NMR spectroscopy. From the ^{1}H NMR spectra it was concluded that ring closure between different hydroquinone units of **2** had occurred. A template effect due to the potassium ion is probably the origin of this feature.

Complexation of Alkali Metal and Ammonium Salts. Because of the presence of receptor sites, it was tempting to complex alkali metal and ammonium salts within the baskets. Using ^{1}H NMR shift experiments we investigated the stoichiometry of complexation of these guest molecules. Specifically, we added small amounts of potassium picrate as a solid to a solution of a basket in $CDCl_3$–DMSO-d_6 (3:1, v/v). These experiments revealed

Chart I

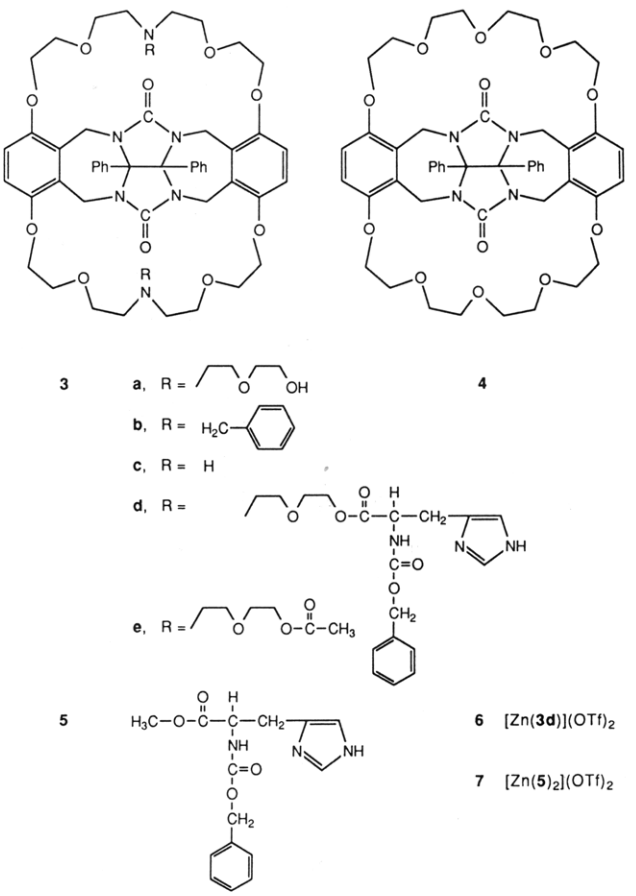

Scheme I

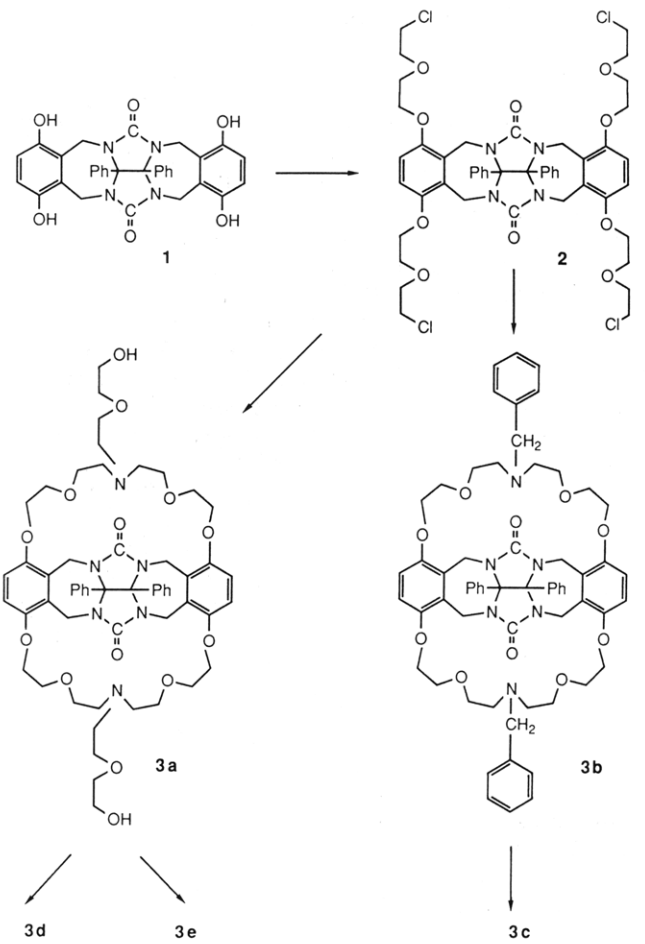

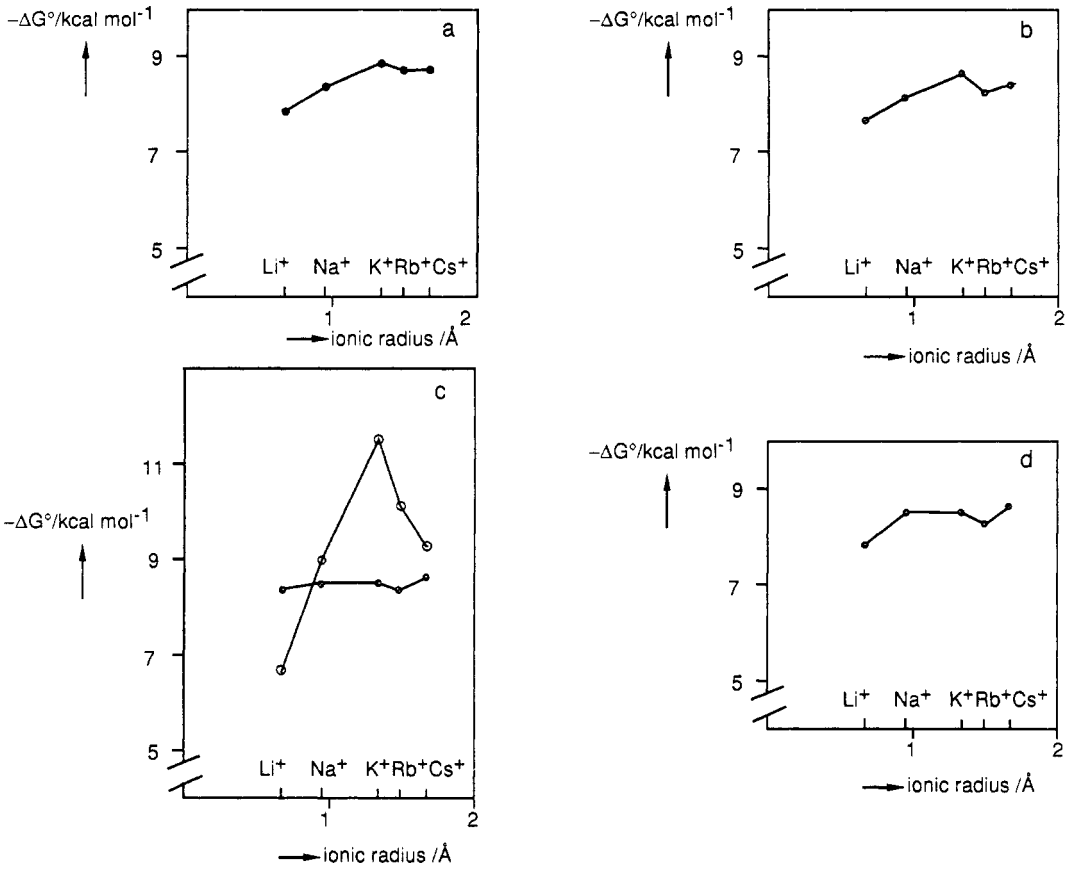

Figure 4. Plots of $-\Delta G°$ value vs the radius of the complexed cation: **3a** (a); **3b** (b); **3c** (o) and **4** (○) (c); **3d** (d).

that baskets **3a–d** form 1:1 complexes with potassium picrate, with slow exchange on the ^1H NMR time scale at room temperature. For example, the hydroquinone protons of the baskets show one signal in the spectrum of the host. Upon adding K^+, a second signal appears at about 10 Hz lower field while the original signal decreases. By the time 1 equiv has been added, the first signal disappears completely and the second one is at its maximum. Upon addition of more than 1 equiv, the spectra do not undergo any further changes. A similar behavior is observed for the AB pattern of the NCH_2Ar protons.

The association constants (K_a) and the free energies of complexation ($-\Delta G°$) between hosts **3a–d** and Li^+, Na^+, K^+, Rb^+, Cs^+, NH_4^+, $CH_3NH_3^+$, and t-$BuNH_3^+$ picrates, in $CHCl_3$ saturated with water, were determined by means of the picrate extraction technique described by Cram et al.[5] They were calculated based on an assumed 1:1 complex formation and are presented in Table I. In Figure 4 the $-\Delta G°$ values are plotted against the ionic radii of the complexed alkali metal ions. For comparison, the values of host **4** in which the R-N units are replaced by oxygen atoms[3b] are also included in Table I and Figure 4c.

Previously, we reported that **4** and alkali metal ions form 1:1 host–guest complexes in which the ion is bound in a clamshell-like fashion.[3b] Since **3a–d** form 1:1 complexes with metal ions as well, it is most likely that a similar kind of conformation is present (Figure 5). If this is true, then the side arms will not have much influence on the binding of the guest, as they are confined to the outside of the shell. The data in Table I and Figure 5 confirm this hypothesis. The differences in the $-\Delta G°$ values are not very large. The presence or absence (**3c**) of a side chain, and whether the

Table I. Association Constants and Free Energies of Binding of Picrate Salt Guests to Hosts at 25 °C in $CHCl_3$ Saturated with H_2O[a]

host	cation of guest	$K_a \times 10^{-6}$, M^{-1}	$-\Delta G°$, kcal mol^{-1}
3a	Li^+	0.62	7.9
	Na^+	1.4	8.4
	K^+	3.2	8.9
	Rb^+	2.3	8.7
	Cs^+	2.3	8.7
	NH_4^+	9.5	9.5
	$CH_3NH_3^+$	0.34	7.5
	t-$BuNH_3^+$	0.02	5.9
3b	Li^+	0.38	7.6
	Na^+	0.83	8.1
	K^+	1.9	8.6
	Rb^+	0.98	8.2
	Cs^+	1.4	8.4
	NH_4^+	3.8	9.0
	$CH_3NH_3^+$	0.27	7.4
	t-$BuNH_3^+$	0.015	5.7
3c	Li^+	1.4	8.4 (6.7)[b]
	Na^+	1.6	8.5 (9.0)[b]
	K^+	1.6	8.5 (11.5)[b]
	Rb^+	1.5	8.4 (10.1)[b]
	Cs^+	2.0	8.6 (9.3)[b]
	NH_4^+	37	10.3 (9.5)[b]
	$CH_3NH_3^+$	1.0	8.2 (8.1)[b]
	t-$BuNH_3^+$	0.12	6.9 (5.5)[b]
3d	Li^+	0.56	7.8
	Na^+	1.7	8.5
	K^+	1.8	8.5
	Rb^+	1.2	8.3
	Cs^+	2.2	8.6
	NH_4^+	9.0	9.5
	$CH_3NH_3^+$	0.36	7.6
	t-$BuNH_3^+$	0.027	6.0

[a] Estimated error in $\Delta G°$ ± 3%. For a discussion of the precision of the picrate extraction technique see ref 5. [b] Free energies of binding of **4**.[3b]

(5) Helgeson, R. C.; Weisman, G. R.; Toner, J. L.; Tarnowski, Th. L.; Chao, Y.; Mayer, J. M.; Cram, D. J. *J. Am. Chem. Soc.* **1979**, *101*, 4928.

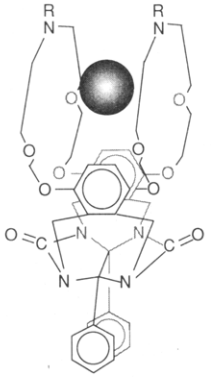

Figure 5. A clamshell-like complex of a basket, the handles of which encapsulate a potassium ion.

Table II. Absorption Maxima of Potassium Picrate Extracted into CH_2Cl_2 with Hosts 3a–d[a]

host	λ_{max}, nm	host	λ_{max}, nm
3a	374	**3d**	373
3b	371	**4**	375
3c	362		

[a] Extraction experiments were carried out with a CH_2Cl_2 solution of the host (10 mL, 0.3 mM) and an aqueous solution of potassium picrate (10 mL, 3.0 mM).

side chains have donor properties (**3a** or **3d**) or not (**3b**) are not factors which substantially affect the $-\Delta G°$ values. In contrast to this finding, Gokel[6a] and Nakatsuji[6b] showed that the presence of side chains at crown ethers (so called lariat ethers) and variations in the structure, and donor group arrangements in these chains can lead to a relatively broad range in both cation binding strengths and selectivities. For example, attachment of a quinoline side arm to 15-crown-5 leads to an increase in the association constant for binding of Na^+ by a factor of 36.[6b]

Compound **3a** displays almost the same binding pattern and binding strengths as basket **3d**, with the exception of the higher value for complexation with K^+ (a difference of 0.4 kcal mol^{-1}). Similar binding patterns are also observed for compounds **3a** and **3b**, but in this case the free energies of binding of the latter are 0.3 kcal mol^{-1} lower for all the guests. Apparently, the side chain with donor ability has a small positive effect on the binding properties when compared with the side chain without this donor ability.

All baskets **3a–d** display a very "flat" pattern for the free energies of binding. This feature is most pronounced in the case of **3c**, which binds all alkali metal ions, even Li^+, with the same $-\Delta G°$ value (within experimental error). It is remarkable that the binding pattern totally changes when the NH in the ring is replaced by an oxygen atom. Compound **4** is much more selective in binding alkali metal ions than **3c** (see Figure 4c).

Baskets **3a–d** are relatively strong binders of the NH_4^+ ion ($-\Delta G°$ = 10.3 kcal mol^{-1} for **3c**). The reason for this is probably the presence of the NH function in the handles. These baskets exhibit the same binding pattern: $NH_4^+ > CH_3NH_3^+ > t\text{-}BuNH_3^+$. This sequence can be explained by steric factors; the *tert*-butyl group is too bulky to fit into the basket.

For the potassium complexes of compounds **3a–d**, the position of the major UV/vis absorption band of the picrate anion in CH_2Cl_2 was determined (Table II). Recently, Inoue et al. have reported that the position of this band gives information as to whether the picrate anion is present as a separated ion pair ($\lambda_{max} \approx 375$ nm) or as a contact ion pair ($\lambda_{max} \approx 360$ nm).[7] For the side chain containing baskets **3a,b,d**, we find values which correspond to separated ion pairs. This finding was anticipated, as the cation is completely encapsulated by the oxyethylene handles of the baskets. The side chains of the baskets may cause additional shielding of the potassium ion. This shielding effect is larger for **3a** (λ_{max} = 374 nm), which has electron-donating side arms, than for **3b** (λ_{max} = 371 nm), which is devoid of this property and which, moreover, is sterically less suited to shield the cation. Compound **3c** gives a λ_{max} that corresponds to a contact ion pair. From this result we conclude that the cation is not as well encapsulated. The absence of side arms could be one reason, but it is not the only one because compound **4**, in which NH is substituted by O, does form a separated ion pair. The reason for this different behavior is not yet clear.

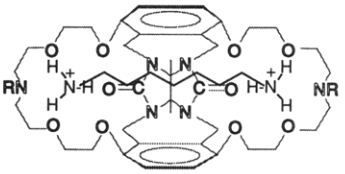

Figure 6. Drawing of an aliphatic diammonium dipicrate salt complexed to a basket. The diammonium guest is wedged in between the *o*-xylylene rings.

Table III. ^1H NMR Chemical Shifts of Guests $^+H_3N(CH_2)_nNH_3^+$, n = 3–9, Added in a 1:1 Ratio to 3a[a]

	guest chemical shifts/ppm				
guest	α	β	γ	δ	ϵ
$^+H_3N(CH_2)_nNH_3^+$					
n = 3	2.34	1.10			
n = 4	2.23	0.40			
n = 5	2.33	0.60	0.11		
n = 6	2.55	0.42	0.21		
n = 7	2.72	1.05	0.51	0.37	
n = 8	2.68[b]	1.17[b]	0.89[b]	0.69[b]	
n = 9	2.74[b]	1.39[b]	1.00[b]	1.08[b]	1.08[b]

[a] ^1H NMR spectra were recorded in $CDCl_3$–DMSO-d_6 (6:1, v/v) at 25 °C. [b] Tentative assignment.

Complexation of Aliphatic and Aromatic Diammonium Salts. The stoichiometry of complexation of aliphatic and aromatic diammonium salts by **3a–d** was determined through ^1H NMR experiments. When each ammonium group of the guest is complexed at one binding site of the host, the aliphatic chain lies in the cavity of the basket (see Figure 6) and is in the shielding zone of the *o*-xylylene units. That this kind of complexation indeed occurs is evidenced by the upfield shifts of the guest protons in the ^1H NMR spectra. In Table III the chemical shifts of the guests $^+H_3N(CH_2)_nNH_3^+$, n = 3–9 are presented; the solid diammonium dipicrate salt has been added in a 1:1 ratio to a solution of host **3a** in the solvent mixture $CDCl_3$–DMSO-d_6 (6:1, v/v) at 25 °C. The largest upfield shifts are observed for the methylene protons in the middle of the $(CH_2)_n$ chain, as they are situated in the center of the shielding zone. For example, the γ protons of pentanediammonium dipicrate display an upfield shift of almost 1.5 ppm upon complexation.

Because of the flexibility of the handles, the host can adapt itself to a particular guest. The same holds true in

(6) (a) Gokel, G. W.; Arnold, K. A.; Delgado, M.; Echeverria, L.; Gatto, V. J.; Gustowski, D. A.; Hernandez, J.; Kaifer, A.; Miller, S. R.; Echegoyen, L. *Pure Appl. Chem.* **1988**, *60*, 461–465 and references therein. (b) Nakatsuji, Y.; Nakamura, T.; Yonetani, M.; Yuya, H.; Okahara, M. *J. Am. Chem. Soc.* **1988**, *110*, 531–538 and references therein.

(7) Inoue, Y.; Fujiwara, C.; Wada, K.; Tai, A.; Hakushi, T. *J. Chem. Soc., Chem. Commun.* **1987**, *6*, 393–394.

reverse for the guest molecules which have flexible aliphatic chains. When the aliphatic chain is short, the handles of the baskets move toward each other; when the chain is long, they move apart. The guest $^+H_3N(CH_2)_nNH_3^+$, $n = 3$, is too short to bind at each side of the basket. This observation is supported by the fact that the upfield shift of the β-methylene protons is very small (Table III). When $n = 4$, the chain is just long enough to form a 1:1 complex; accordingly, the β-CH_2 protons are shifted to 0.40 ppm. It can be concluded from Table III that the CH_2 protons of the long-chain guests (see, for example, the last entry) are not situated in the shielding zone of the building block. For these guests, there are two possibilities for complexation: a 1:1 complex, in which case the $(CH_2)_n$ chain is folded outside the cavity (because it is too long to be stretched out completely), or a 2:2 complex, in which case one of the ammonium groups is bound in one basket and the other in a second basket.

On the ^1H NMR time scale, the exchange of the diammonium salts is rapid at room temperature. This can be concluded from the fact that only average methylene proton signals from the complexed and noncomplexed salt are present when the salt is added in a 2:1 ratio with respect to the host.

The association constants and free energies of binding for the complexes between **3a–d** and 11 diammonium guests were determined by the extraction method in $CHCl_3$ saturated with water at 25 °C.[3b,c] In the calculation of the K_a and $-\Delta G°$ values (Table IV), a 1:1 stoichiometry was assumed for the complexes between hosts **3a–d** and $^+H_3N(CH_2)_nNH_3^+$, $n = 3$–9, dipicrate salts, *m*- and *p*-xylylenediammonium dipicrate salts, and *o*- and *p*-phenylenediammonium dipicrate salts. The K_a and $-\Delta G°$ values in Table IV must be considered lower limits, because the distribution constant of the uncomplexed guest between $CHCl_3$ and H_2O could not be measured accurately.[3b,c]

The binding profiles of compounds **3a–d** with aliphatic diammonium salts are very flat, probably because the baskets easily adapt to the guest, as outlined above.

In all the compounds **3a–d**, the binding of butanediammonium is somewhat stronger than that of the other aliphatic diammonium salts. The reason for this effect is not yet clear.

For guests with $n \geq 5$ the $-\Delta G°$ values of compound **4** are higher ($\approx$1.5 kcal mol^{-1}) than those of **3c**. For **4** the maximum $-\Delta G°$ value is reached when $n = 6$, whereas for **3c** the binding profile remains flat. It is surprising that replacement of only one oxygen by NH leads to such large differences.

Table IV shows that the binding constants of **3a–d** with $^+H_3N(CH_2)_nNH_3^+$, $n = 3$, are higher than the corresponding binding constant of **4** with this guest. This can be explained in the following way: The pK_a values of $^+H_3N(CH_2)_nNH_3^+$, $n = 3$, are 9.03 and 10.94.[8] This difference in pK_a is caused by the electrostatic repulsion of the two ammonium groups, which are situated close to each other. As the chain length increases, this difference decreases. When this guest binds to the host, the electrostatic repulsion can be diminished by transfer of a proton from one ammonium group to a tertiary nitrogen in a ring of the basket. That proton transfer indeed occurs can be concluded from ^1H NMR experiments. Table III reveals a gradual shift of the α-protons from δ 2.3 when $n = 3$ to δ 2.7 ppm when $n = 9$. These shifts indicate that for $n = 3$, proton transfer is appreciable, while for $n = 9$ it is small.

(8) Weast, R. C. *CRC Handbook of Chemistry and Physics*, 58th ed.; CRC Press: Palm Beach, 1978; p D-148.

Table IV. Association Constants and Free Energies of Binding of Diammonium Dipicrate Salts to Hosts at 25 °C in $CHCl_3$ Saturated with H_2O[a]

host	cation of guest	$K_a \times 10^{-8}$,[b] M^{-1}	$-\Delta G°$, kcal mol^{-1}
3a	$^+H_3N(CH_2)_nNH_3^+$		
	$n = 3$	1.9	11.3
	$n = 4$	4.8	11.8
	$n = 5$	2.3	11.4
	$n = 6$	2.8	11.5
	$n = 7$	2.5	11.4
	$n = 8$	3.7	11.7
	$n = 9$	4.0	11.7
	p-xylylenediammonium	33	13.0
	m-xylylenediammonium	21	12.7
	p-phenylenediammonium	52	13.3
	o-phenylenediammonium	5.5×10^3	16.0
3b	$^+H_3N(CH_2)_nNH_3^+$		
	$n = 3$	1.5	11.2
	$n = 4$	3.4	11.6
	$n = 5$	1.3	11.1
	$n = 6$	2.1	11.3
	$n = 7$	2.3	11.4
	$n = 8$	2.3	11.4
	$n = 9$	2.8	11.5
	p-xylylenediammonium	18	12.6
	m-xylylenediammonium	10	12.3
	p-phenylenediammonium	1.4×10^2	13.8
	o-phenylenediammonium	1.3×10^4	16.5
3c	$^+H_3N(CH_2)_nNH_3^+$		
	$n = 3$	8.4	12.2 ($\approx$9.5)[c]
	$n = 4$	19	12.6 (11.3)[c]
	$n = 5$	5.0	11.9 (12.6)[c]
	$n = 6$	6.4	12.0 (13.3)[c]
	$n = 7$	5.9	12.0 (13.3)[c]
	$n = 8$	6.5	12.0 (13.3)[c]
	$n = 9$	6.5	12.0 (13.5)[c]
	p-xylylenediammonium	2.6×10^2	14.2 (12.8)[c]
	m-xylylenediammonium	1.2×10^2	13.7 (12.7)[c]
	p-phenylenediammonium	0.66×10^2	13.4 (11.4)[c]
	o-phenylenediammonium	3.5×10^4	17.1 (12.3)[c]
3d	$^+H_3N(CH_2)_nNH_3^+$		
	$n = 3$	2.6	11.5
	$n = 4$	6.0	12.0
	$n = 5$	1.4	11.1
	$n = 6$	2.5	11.4
	$n = 7$	2.3	11.4
	$n = 8$	2.8	11.5
	$n = 9$	3.4	11.6
	p-xylylenediammonium	35	13.0
	m-xylylenediammonium	17	12.6
	p-phenylenediammonium	48	13.2
	o-phenylenediammonium	2.2×10^5	$\approx$18

[a] See Experimental Section for methods. Estimated error in $\Delta G° \pm 3\%$. [b] The values have been calculated assuming a distribution constant K_d of 1 M^{-1}; they are considered to be lower limits.[3c] [c] Free energies of binding of **4**.[3b]

The free energies of binding of compounds **3a–d** with aromatic diammonium salts are higher than those of **4**. The most interesting feature is the extremely high $-\Delta G°$ value observed for the binding of *o*-phenylenediammonium salt (as high as 18 kcal mol^{-1} for **3d**). An explanation similar to that advanced for the binding of the propanediammonium salt can be invoked in this case. In *o*-phenylenediammonium, the two NH_3^+ groups are again close to each other, and, therefore, proton transfer will relieve repulsion. In the ^1H NMR spectrum, the CH_2 protons adjacent to the nitrogen in the ring of the free host **3a** are seen at 2.75 ppm in $CDCl_3$–DMSO-d_6 (6:1, v/v). When the *o*-phenylenediammonium salt is complexed to this host, these protons shift downfield to 3.2 ppm. This downfield shift signals that proton transfer from the guest to a tertiary amine of the host has occurred.

Receptors for diammonium salts have also been synthesized by Sutherland[9] and by Lehn.[10] These receptors

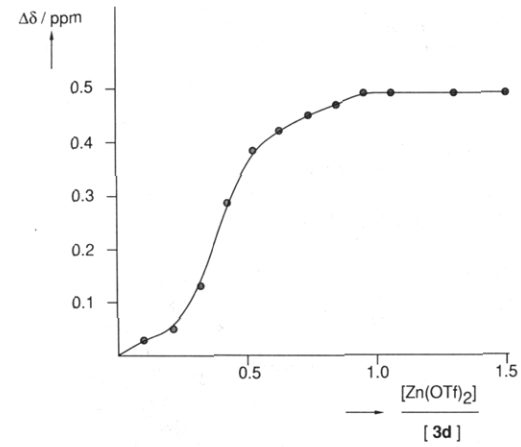

Figure 7. Stoichiometry of complexation of $Zn(OTf)_2$ to **3d**: the ratio $[Zn(OTf)_2]/[\mathbf{3d}]$ vs induced chemical shift ($\Delta\delta$) of the NCH N imidazolyl proton signals.

(which are cylindrically shaped) consist of two diaza- and triazacrown ethers, which are held in a more or less coplanar arrangement by lateral bridges. The bridges include flexible oxyethylene chains as well as rigid aromatic rings. On complexation of a diammonium guest, the receptors containing the latter rings show upfield shifts in the ^1H NMR spectra similar to those of our baskets. They are also reported to display selective binding, with the highest selectivities being observed for the cylinders with the most defined cavities. Unfortunately, no association constants have been published for these receptor molecules; therefore, a comparison with our compounds is not possible. Our feeling is that the selectivities displayed by **3a–d** for aliphatic diammonium guests are lower than those displayed by the above-mentioned cylinders with rigid aromatic bridges. They are more like the selectivities displayed by the cylinders with oxyethylene bridges. On the other hand, our baskets seem to be more selective toward aromatic diammonium guests. More data, however, will be required in order to substantiate this assertion.

Synthesis of a Zinc Complex of Compound 3d. Compound **3d** contains two histidine residues which could complex a metal center. In the present study we have chosen to use a Zn(II) ion as a test case.

First, a ^1H NMR titration experiment was performed. $Zn(OTf)_2$ (OTf^- = triflate anion), dissolved in $CDCl_3$–DMSO-d_6 (3:1, v/v) was added in small parts to a solution of **3d** in the same solvent mixture. The chemical shifts of the imidazolyl protons of **3d** were examined as a function of added amount of Zn(II) ions. The results are presented in Figure 7. The three inflection points indicate that the stoichiometry of the complex depends on the concentration of the Zn(II) ions. The inflection point at approximately 0.25 equiv could not be interpreted. When 0.5 equiv of $Zn(OTf)_2$ is added to **3d**, complexes are formed in which four imidazole groups coordinate to one Zn(II) ion. Upon addition of another 0.5 equiv of Zn(II), the stoichiometry changes to two imidazole groups coordinated to one Zn(II) ion. It is most likely that in the former case two host molecules complex one molecule of $Zn(OTf)_2$. In the latter case, we propose that an internal 1:2 Zn–imidazole complex (ligand **3a**–$Zn(OTf)_2$ = 1:1) is formed. From the literature it is known that zinc(II) can form all kinds of coordination complexes (tetrahedral, distorted trigonal-bipyramidal, square-pyramidal, and octahedral), depending on both the concentration and nature of the ligand.[2b,11]

Table V. Molar Conductivities of Zinc Complexes[a]

compound	Λ_m, Ω^{-1} cm^2 mol^{-1}
$[Zn(\mathbf{3d})](OTf)_2$	88
$[Zn(\mathbf{5})_2](OTf)_2$	78
$Zn(OTf)_2$	73
	141[b]
	180[c]
TEBA[d]	77

[a] In $CHCl_3$–CH_3OH (1:1, v/v) at 25 °C, 10^{-3} M. Estimated error in molar conductivity ±5%. [b] In acetone–CH_3OH (20:1, v/v). [c] In CH_3OH. [d] TEBA = triethylbenzylammonium chloride.

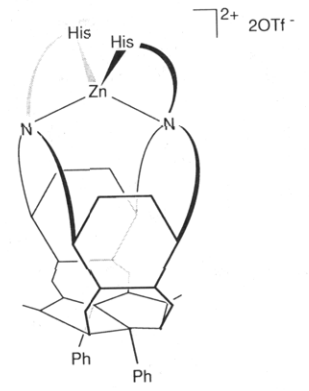

Figure 8. Schematic representation of $[Zn(\mathbf{3d})](OTf)_2$.

For comparison, a similar ^1H NMR experiment was carried out with the model compound *N*-(benzyloxycarbonyl)-L-histidine methyl ester (Z-L-His-OCH_3) (**5**). In this case as well we found stoichiometries which depended on the Zn(II) concentration: a 1:4 Zn–imidazole complex and a 1:2 Zn–imidazole complex. Thus, the stoichiometries of both **3d** and **5** with Zn(II) correspond to each other.

The $Zn(OTf)_2$ complexes of **3d** and **5** were synthesized by adding 1 equiv of $Zn(OTf)_2$ to 1 equiv of **3d** in $CHCl_3$–CH_3OH (8:2, v/v) and to 2 equiv of **5** in $CHCl_3$.

Attempts to measure FAB MS spectra of $[Zn(\mathbf{3d})](OTf)_2$ were not successful. For $[Zn(\mathbf{5})_2](OTf)_2$ a FAB MS spectrum could be obtained in *m*-nitrobenzyl alcohol. A large signal was present at m/z 819 ($[Zn(\mathbf{5})_2](OTf)^{\bullet+}$) and a small one at m/z 969 ($[Zn(\mathbf{5})_2](OTf)_2 + H)^{\bullet+}$. These two signals indicate that the Zn(II) ion is coordinated by two histidine groups.

Gel permeation chromatography was performed in order to obtain information on the relative molecular sizes of the complexes. By comparing the elution time of $[Zn(\mathbf{3d})](OTf)_2$ with that of the free ligand **3d**, we could ascertain whether the complex was monomeric or oligomeric. The observed difference of only half a minute (27 min for $[Zn(\mathbf{3d})](OTf)_2$ and 26.5 min for **3d**) indicates that the molecular size of the two compounds is of the same order of magnitude. It is therefore concluded that $[Zn(\mathbf{3d})](OTf)_2$ is monomeric.

Molar conductivities of the zinc complexes are presented in Table V. The conductivities of $[Zn(\mathbf{3d})](OTf)_2$ and $[Zn(\mathbf{5})_2](OTf)_2$ lie in the range of the conductivity of $Zn(OTf)_2$. The somewhat higher conductivity of $[Zn(\mathbf{3d})](OTf)_2$ is probably due to the steric shielding of the Zn(II) ion by the ligand.

The exact nature of the coordination sphere around the Zn(II) ion in $[Zn(\mathbf{3d})](OTf)_2$ is difficult to determine

(9) Sutherland, I. O. *Chem. Soc. Rev.* **1986**, *15*, 63–91.
(10) (a) Hamilton, A.; Lehn, J. M.; Sessler, J. L. *J. Am. Chem. Soc.* **1986**, *108*, 5158–5167. (b) Dietrich, B. In *Inclusion compounds*; Atwood, J. L., Davies, J. E. D., MacNicol, D. D., Eds.; Academic Press: New York, 1984; Vol. 2, pp 363–366.
(11) (a) Eichhorn, G. L. *Inorganic Biochemistry*; Elsevier: Amsterdam, 1973; Vol. 1, p 25. (b) Sigel, H. *Metal Ions in Biological Systems*; Marcel Dekker Inc.: New York, 1973; Vol. 2, p 33.

without an X-ray structure. It is most likely that, aside from the two imidazolyl groups, the tertiary nitrogen atoms in the ring of ligand **3d** also coordinate to the zinc atom (see Figure 8). This suggestion is confirmed by the fact that the protons of the CH_2N groups shift downfield upon complexation of zinc(II), viz from 2.8 ppm in the free ligand **3d** to >3.3 ppm in the complex. The latter value could not be determined exactly as the signals of interest are masked by the AA'BB' signals of the oxyethylene chains of the ligand.

Conclusion

The work presented herein demonstrates that host molecules containing a metal center as well as a cavity for the binding of substrates are accessible in good yields from building block **1**. Our current research is directed toward catalytic application of our systems using zinc, copper, and rhodium as the metal centers.

Experimental Section

General. Unless otherwise indicated, commercial materials were used as received. DMSO and DMF were dried over 4-Å sieves, and methanol over 3-Å sieves prior to use. Diethyl ether and toluene were distilled from sodium benzophenone and ketyl, $CHCl_3$ was distilled from $CaCl_2$. FAB mass spectra were recorded on a VG ZAB 2F spectrometer (matrix: *m*-nitrobenzyl alcohol and triethyl citrate). ^1H NMR spectra were recorded at 60, 80, or 200 MHz. Conductivity measurements were carried out at 25.0 °C using a Philips PW 9501 conductivity meter. For determination of relative molecular sizes, gel permeation chromatography was performed on a Sephadex LH-20 column (length 21.5 cm, diameter 1 cm) with $CHCl_3$–CH_3OH (9:1, v/v) as eluent at a flow rate of 20 mL/h. Silica gel 60 (Merck, particle size 0.040–0.063 mm, 230–400 mesh, ASTM), neutral alumina (Janssen, active, 50–200 μm, 70–290 mesh, ASTM) and Sephadex LH-20 (Pharmacia) were used in column chromatography. Thin-layer chromatography was performed with plates of silica gel 60 F254 (Merck) and alumina (Merck, neutral, type E).

1,3:4,6-Bis(3,6-dihydroxy-1,2-xylylene)tetrahydro-3a,6a-diphenylimidazo[4,5-*d*]imidazole-2,5(1*H*,3*H*)-dione (1). This compound was synthesized according to a procedure developed in our laboratory.[3]

1,3:4,6-Bis[3,6-bis(6-chloro-1,4-dioxahexyl)-1,2-xylylene]-tetrahydro-3a,6a-diphenylimidazo[4,5-*d*]imidazole-2,5-(1*H*,3*H*)-dione (2). This compound was synthesized according to a procedure developed in our laboratory.[3c]

1,3:4,6-Bis{3,3':6,6'-bis[1,4,10,13-tetraoxa-7-(5-hydroxy-3-oxapent-1-yl)-7-azatridecamethylene]-1,2-xylylene}tetrahydro-3a,6a-diphenylimidazo[4,5-*d*]imidazole-2,5(1*H*,3*H*)-dione (3a). A mixture of 3.0 g (3.04 mmol) of **1**, 1.58 g (15.0 mmol) of 2-(2-aminoethoxy)ethanol, 15 g of potassium carbonate, and a tiny amount of potassium iodide in 150 mL of DMSO was stirred at 100 °C under a nitrogen atmosphere. After cooling, the reaction mixture was poured into 450 mL of water. The resulting precipitate was collected by filtration over infusorial earth, dissolved in $CHCl_3$, and washed four times with water. The solution was evaporated under reduced pressure, and the crude product was stirred in diethyl ether. After filtration, the light yellow solid was purified by column chromatography (Sephadex LH-20, eluent $CHCl_3$). Yield 1.28 g (40%) of **3a**: mp >195 °C dec; IR (KBr) 3600–3200 (OH), 2960–2850 (CH_2), 1705 (C=O), 1590 (aromatic C=C), 1480–1410 (CH_2), 1150–1050 (COC) cm^{-1}; ^1H NMR ($CDCl_3$) δ 7.02 (s, 10 H, ArH), 6.67–6.37 (m, 4 H, ArH), 5.67 (d, 4 H, NC*H*HAr, *J* = 16 Hz), 4.40–3.13 (m, 42 H, CH_2O, OH, NCH*H*Ar), 3.13–2.67 (m, 12 H, NCH_2CH_2O); ^1H NMR ($CDCl_3$) δ 6.67–6.37 (m, 4 H, ArH) changes into δ 6.65 (s, 4 H, ArH) after addition of 3 drops of CD_3OD; FAB MS (*m*-nitrobenzyl alcohol) *m/z* 1053 $(M + H)^+$, 1071 $(M + H_2O + H)^+$. Anal. Calcd for $C_{56}H_{72}N_6O_{14}\cdot(H_2O)_{2.3}$: C, 61.71; H, 6.66; N, 7.71; O, 23.92. Found: C, 61.63; H, 6.78; N, 7.64; O, 23.89.

1,3:4,6-Bis[3,3':6,6'-bis(1,4,10,13-tetraoxa-7-benzyl-7-azatridecamethylene)-1,2-xylylene]tetrahydro-3a,6a-diphenylimidazo[4,5-*d*]imidazole-2,5(1*H*,3*H*)-dione (3b). This compound was synthesized from **2** (3.0 g, 3.04 mmol) and benzylamine (1.62 g, 15.1 mmol) as described for **3a**. Yield 1.67 g (52%) of **3b** as a light yellow solid: mp >185 °C dec; IR (KBr) 3080–2980 (ArH), 2960–2840 (CH_2), 1705 (C=O), 1640–1590 (aromatic C=C), 1480–1420 (CH_2), 1150–1050 (COC) cm^{-1}; ^1H NMR ($CDCl_3$) δ 7.20 (s, 10 H, ArH), 7.02 (s, 10 H, ArH), 6.73–6.23 (m, 4 H, ArH), 5.67 (d, 4 H, NC*H*HAr, *J* = 16 Hz), 4.45–3.33 (m, 32 H, CH_2O, $PhCH_2N$, NCH*H*Ar), 3.10–2.68 (m, 8 H, OCH_2CH_2N); FAB MS (*m*-nitrobenzyl alcohol) *m/z* 1057 $(M + H)^+$. Anal. Calcd for $C_{62}H_{68}N_6O_{10}$: C, 70.44; H, 6.48; N, 7.95; O, 15.13. Found: C, 70.43; H, 6.29; N, 7.80; O, 15.48.

1,3:4,6-Bis[3,3':6,6'-bis(1,4,10,13-tetraoxa-7-azatridecamethylene)-1,2-xylylene]tetrahydro-3a,6a-diphenylimidazo-[4,5-*d*]imidazole-2,5(1*H*,3*H*)-dione (3c). A mixture of 0.35 g (0.33 mmol) of **3b** and a catalytic amount of 10% Pd/C in 40 mL of acetic acid was stirred at 55 °C for 168 h under 4 atm of hydrogen gas. The reaction mixture was filtered over infusorial earth, and the filtrate was evaporated to dryness under reduced pressure. Traces of acetic acid were removed by codistillation with toluene (2 × 10 mL). The remaining solid was dissolved in $CHCl_3$ and washed with acidic water (pH was adjusted to 1 with concentrated hydrochloric acid), with basic water (pH of 12 with potassium carbonate), and four times with water to neutral pH. The solvent was evaporated under reduced pressure to yield 204 mg (70%) of pure **3c**: mp >200 °C dec; IR (KBr) 3310 (NH), 2980–2850 (CH_2), 1705 (C=O), 1600 (aromatic C=C), 1500–1420 (CH_2), 1150–1050 (COC) cm^{-1}; ^1H NMR ($CDCl_3$) δ 7.02 (s, 10 H, ArH), 6.42 (s, 4 H, ArH), 5.67 (d, 4 H, NC*H*HAr, *J* = 16 Hz), 4.45–3.17 (m, 28 H, CH_2O, NCH*H*Ar), 3.17–2.57 (m, 8 H, OCH_2CH_2N); FAB MS (triethyl citrate and *m*-nitrobenzyl alcohol) 877 $(M + H)^+$, 893 $(M + H_2O + H)^+$. Anal. Calcd for $C_{48}H_{56}N_6O_{10}$: C, 68.34; H, 5.95; N, 8.85; O, 16.86. Found: C, 68.14; H, 6.04; N, 8.72; O, 17.10.

1,3:4,6-Bis{3,3':6,6'-bis[1,4,10,13-tetraoxa-7-(5-(*N*-(benzyloxycarbonyl)-L-histidyl)-3-dioxapent-1-yl)-7-azatridecamethylene]-1,2-xylylene}tetrahydro-3a,6a-diphenylimidazo-[4,5-*d*]imidazole-2,5(1*H*,3*H*)-dione (3d). A mixture of 0.22 g (0.209 mmol) of **3a** and 0.141 mg (0.473 mmol) of *N*-(benzyloxycarbonyl)-L-histidine was dissolved in anhydrous DMF under a nitrogen atmosphere. The solution was cooled to 0 °C, and 0.11 g (0.55 mmol) of *N,N*-dicyclohexylcarbodiimide was added. The mixture was stirred for 2 h at this temperature and subsequently for 16 h at room temperature. The reaction mixture was filtered and evaporated under high vacuum at 30 °C, and the residue was dissolved in chloroform. The chloroform layer was filtered, washed with basic water (potassium carbonate solution), a few times with water, and evaporated under reduced pressure. The product was purified by column chromatography (Sephadex LH-20, eluent $CHCl_3$). Yield 0.15 g (45.5%) of **3d**: mp >165 °C dec; IR (KBr) 3500–3100 (NH), 1770–1650 (C=O), 1100–1030 (COC) cm^{-1}; ^1H NMR ($CDCl_3$) δ 7.3 (s, 10 H, CH_2ArH), 7.2 (m, 2 H, NC*H*N), 7.05 (s, 10 H, ArH), 6.9–6.1 (m, 6 H, ArH, NC*H*C), 5.6 (d, 4 H, NC*H*HAr, *J* = 16 Hz), 5.1 (s, 4 H, CH_2Ar), 4.5 (m, 2 H, C(O)-C*H*NH), 4.4–3.2 (m, 44 H, OCH_2, NCH*H*Ar), 3.2–2.7 (m, 16 H, CH_2Im, CH_2N); FAB MS (*m*-nitrobenzyl alcohol) *m/z* 1595 $(M + H)^+$, 1613 $(M + H_2O + H)^+$, 1631 $(M + 2H_2O + H)^+$, 1540 $(M + 2H_2O - CH_2Ph + H)^+$, 1522 $(M + H_2O - CH_2Ph + H)^+$, 1386 $(M + 2H_2O - C_{13}H_{15}N_3O_2 + H)^+$, 1053 $(M - 2Z\text{-L-His} + H)^+$. Anal. Calcd for $C_{84}H_{98}N_{12}O_{20}\cdot 5H_2O$: C, 59.85; H, 6.41; N, 9.97; O, 23.75. Found: C, 59.92; H, 6.53; N, 9.84; O, 23.71.

1,3:4,6-Bis{3,3':6,6'-bis[1,4,10,13-tetraoxa-7-(5-acetoxy-3-oxapent-1-yl)-7-azatridecamethylene]-1,2-xylylene}tetrahydro-3a,6a-diphenylimidazo[4,5-*d*]imidazole-2,5(1*H*,3*H*)-dione (3e). A mixture of 0.75 g (0.71 mmol) of unpurified **3a** and 1 mL of pyridine in 10 mL of acetic anhydride was stirred at 80 °C for 1.5 h under N_2. The solvent was evaporated under reduced pressure. The residue was dissolved in $CHCl_3$ and washed with basic water (pH 12 with potassium carbonate). The solvent was evaporated. Traces of acetic acid, acetic anhydride, and water in the residue were removed by codistillation with a few milliliters of toluene. The solid material was stirred in diethyl ether, collected by filtration, and dried for 1 day under high vacuum. The remaining light brown solid was chromatographed over Sephadex LH-20 (eluent $CHCl_3$) to yield 0.32 g (40%) of white **5**, partly as a complex with acetic anhydride: mp >190 °C dec; IR (KBr) 2980–2840 (CH_2), 1730 ($C(O)CH_3$), 1705 (C=O), 1490–1410 (CH_2), 1150–1000 (COC) cm^{-1}; ^1H NMR ($CDCl_3$) δ 6.90 (s, 10 H, ArH),

6.52 (s, 4 H, ArH), 5.62 (d, 4 H, NCHHAr, J = 16 Hz), 4.30–3.10 (m, 40 H, CH_2O, NCHHAr), 3.10–2.63 (m, 12 H, NCH_2CH_2O), 2.05 (s, probably complexed acetic anhydride), 2.0 (s, 6 H, CH_3); FAB MS (triethyl citrate) m/z 1137 $(M + H)^+$, 1239 (M + H + acetic anhydride)$^+$.

***N*-(Benzyloxycarbonyl)-L-histidine Methyl Ester (5).** To a solution of 0.97 g (3.24 mmol) of *N*-(benzyloxycarbonyl)-L-histidine in 25 mL of methanol under a nitrogen atmosphere was added 0.82 g (3.97 mmol) of *N,N*-dicyclohexylcarbodiimide at 0 °C. The mixture was stirred for 2 h at this temperature and for 24 h at room temperature. Thereafter, the reaction mixture was filtered, evaporated to dryness, dissolved in CH_2Cl_2, filtered again, and added dropwise to diethyl ether. This mixture was filtered and evaporated to dryness under reduced pressure. The crude product was purified by column chromatography (silica, eluent $CHCl_3$–CH_3OH (95:5, v/v)). Yield 0.35 g (36%) of pure **5**: IR (NaCl) 1770–1630 (C=O), 1100–1000 (COC) cm^{-1}; ^1H NMR ($CDCl_3$) δ 7.5 (s, 5 H, ArH), 7.3 (s, 5 H, ArH), 6.7 (s, 1 H, NCHC), 6.3 (m, 1 H, NHIm), 5.05 (s, 2 H, CH_2Ar), 3.60 (s, 3 H, OCH_3), 3.05 (d, 2 H, CH_2Im); FAB MS (*m*-nitrobenzyl alcohol) m/z 304 $(M + H)^+$. Anal. Calcd for $C_{15}H_{17}N_3O_4$: C, 59.40; H, 5.61; N, 13.86; O, 21.12. Found: C, 59.08; H, 5.72; N, 13.86; O, 21.34.

[Zn(3d)](OTf)$_2$ (6). To a solution of 51 mg (0.032 mmol) of **3d** in 1 mL of $CHCl_3$–CH_3OH (4:1, v/v) was added a solution of 11.2 mg (0.031 mmol) of $Zn(OTf)_2$ in the same solvent mixture. The solution was vortexed for 1 min and added dropwise to diethyl ether. The solid that precipitated was filtered and dried under high vacuum at room temperature. Yield 44.3 mg (70%) of pure **6**: mp >215 °C dec; IR (KBr) 1770–1650 (C=O), 1300, 1160, 1025, 630 ($Zn(OTf)_2$), 1100–1040 (COC) cm^{-1}; ^1H NMR ($CDCl_3/CD_3OD$, 1:1 v/v) δ 7.9 (m, 2 H, NCH), 7.3 (s, 10 H, CH_2ArH), 7.1 (s, 10 H, ArH), 6.9–6.4 (m, 6 H, NCHC, ArH), 5.6 (d, 4 H, NCHHAr), 5.05 (s, 4 H, CH_2Ar), 4.9–3.0 (m, 50 H, C(O)CHNH, OCH_2, NCHHAr, NH, CH_2Im), 2.8 (m, 12 H, CH_2N). Anal. Calcd for $C_{86}H_{98}N_{12}O_{26}ZnF_6S_2$: C, 52.73; H, 5.01; N, 8.58. Found: C, 52.76; H, 5.21; N, 8.35.

[Zn(Z-L-HisOCH$_3$)$_2$](OTf)$_2$ (7). A solution of 66.9 mg (0.22 mmol) of **5** and 38.1 mg (0.105 mmol) of $Zn(OTf)_2$ in 1 mL of $CHCl_3$ was added dropwise to diethyl ether and stirred for 0.5 h at ambient temperature. The solvent was decanted from the sticky solid, and the residue was taken up in chloroform. The resulting suspension was evaporated to dryness to yield 67.5 mg (74%) of pure **7**: IR (KBr) 1770–1650 (C=O), 1300, 1160, 1025, 630 ($Zn(OTf)_2$), 1100–1040 (COC) cm^{-1}; ^1H NMR ($CDCl_3/CD_3OD$, 1:1 v/v) δ 8.0 (s, 1 H, NCHN), 7.3 (s, 5 H, ArH), 6.9 (s, 1 H, NCHC), 5.0 (s, 2 H, CH_2Ar), 4.5 (m, 1 H, CH_2CHNH), 3.7 (s, 3 H, OCH_3), 3.1 (m, 2 H, CH_2Im); FAB MS (*m*-nitrobenzyl alcohol) m/z 969 $(M + H)^+$, 819 $(M - OTf^-)^+$, 516 $(M - 5 - OTf^-)^+$. Anal. Calcd for $C_{32}H_{34}N_6O_{14}ZnF_6S_2$: C, 39.62; H, 3.53; N, 8.66; F, 11.75. Found: C, 40.01; H, 3.62; N, 8.85; F, 11.57.

Determination of K_a and $-\Delta G°$ Values. The technique in which the picrate salt is extracted from H_2O into $CHCl_3$, described by Cram et al.[5], was applied to determine K_a and $-\Delta G°$ values. All these values were calculated and recorded as 1:1 complexes (Table I and Table IV). The extraction experiments involving diammonium dipicrate salts differed slightly from Cram's technique. Instead of 0.015 M host and guest solutions, 0.001 M solutions were used, and instead of 10 μL, 75 μL each of the organic and aqueous phases were diluted to 5 mL with CH_3CN. The equations used to calculate the K_a values in Table IV were reported previously by us.[3c]

Acknowledgment. We thank Prof. W. Drenth for helpful discussions and C. Versluis for recording the FAB mass spectra. This work was supported by the Netherlands Foundation for Chemical Research (SON) with the financial aid from the Netherlands Foundation for Scientific Research (NWO).

Registry No. 1, 106319-02-2; 2, 118715-67-6; **3a**, 124042-44-0; **3a** lithium picrate, 124043-10-3; **3a** sodium picrate, 124043-12-5; **3a** potassium picrate, 124043-14-7; **3a** rubidium picrate, 124043-16-9; **3a** cesium picrate, 124043-18-1; **3a** ammonium picrate, 124042-48-4; **3a** methylammonium picrate, 124042-49-5; **3a** *tert*-butylammonium picrate, 124042-50-8; **3a** propanediammonium dipicrate, 124042-61-1; **3a** butanediammonium dipicrate, 124042-62-2; **3a** pentanediammonium dipicrate, 124042-63-3; **3a** hexanediammonium dipicrate, 124042-64-4; **3a** heptanediammonium dipicrate, 124042-65-5; **3a** octanediammonium dipicrate, 124042-66-6; **3a** nonanediammonium dipicrate, 124042-67-7; **3a** *p*-xylylenediammonium dipicrate, 124042-68-8; **3a** *m*-xylylenediammonium dipicrate, 124042-69-9; **3a** *p*-phenylenediammonium dipicrate, 124042-70-2; **3a** *o*-phenylenediammonium picrate, 124042-71-3; **3b**, 124042-45-1; **3b** lithium picrate, 124043-20-5; **3b** sodium picrate, 124043-22-7; **3b** potassium picrate, 124043-24-9; **3b** rubidium picrate, 124043-26-1; **3b** cesium picrate, 124043-28-3; **3b** ammonium picrate, 124042-51-9; **3b** methylammonium picrate, 124042-52-0; **3b** *tert*-butylammonium picrate, 124042-53-1; **3b** propanediammonium dipicrate, 124042-72-4; **3b** butanediammonium dipicrate, 124042-73-5; **3b** pentanediammonium dipicrate, 124042-74-6; **3b** hexanediammonium dipicrate, 124042-75-7; **3b** heptanediammonium dipicrate, 124042-76-8; **3b** octanediammonium dipicrate, 124042-77-9; **3b** nonanediammonium dipicrate, 124042-78-0; **3b** *p*-xylylenediammonium dipicrate, 124042-79-1; **3b** *m*-xylylenediammonium dipicrate, 124042-80-4; **3b** *p*-phenylenediammonium dipicrate, 124042-81-5; **3b** *o*-phenylenediammonium dipicrate, 124042-82-6; **3c**, 124042-46-2; **3c** lithium picrate, 124043-30-7; **3c** sodium picrate, 124043-32-9; **3c** potassium picrate, 124043-34-1; **3c** rubidium picrate, 124043-36-3; **3c** cesium picrate, 124043-38-5; **3c** ammonium picrate, 124042-54-2; **3c** methylammonium picrate, 124042-55-3; **3c** *tert*-butylammonium picrate, 124042-56-4; **3c** propanediammonium dipicrate, 124042-83-7; **3c** butanediammonium dipicrate, 124042-84-8; **3c** pentanediammonium dipicrate, 124042-85-9; **3c** hexanediammonium dipicrate, 124042-86-0; **3c** heptanediammonium dipicrate, 124042-87-1; **3c** octanediammonium dipicrate, 124042-88-2; **3c** nonanediammonium dipicrate, 124042-89-3; **3c** *p*-xylylenediammonium dipicrate, 124042-90-6; **3c** *m*-xylylenediammonium dipicrate, 124042-91-7; **3c** *p*-phenylenediammonium dipicrate, 124042-92-8; **3c** *o*-phenylenediammonium dipicrate, 124042-93-9; **3d**, 124042-57-5; **3d** lithium picrate, 124043-42-1; **3d** sodium picrate, 124043-44-3; **3d** potassium picrate, 124043-46-5; **3d** rubidium picrate, 124043-48-7; **3d** cesium picrate, 124043-50-1; **3d** ammonium picrate, 124042-58-6; **3d** methylammonium picrate, 124042-59-7; **3d** *tert*-butylammonium picrate, 124042-60-0; **3d** butanediammonium dipicrate, 124042-95-1; **3d** pentanediammonium dipicrate, 124042-96-2; **3d** hexanediammonium dipicrate, 124042-97-3; **3d** heptanediammonium dipicrate, 124042-98-4; **3d** octanediammonium dipicrate, 124042-99-5; **3d** nonanediammonium dipicrate, 124043-00-1; **3d** *p*-xylylenediammonium dipicrate, 124043-01-2; **3d** *m*-xylylenediammonium dipicrate, 124043-02-3; **3d** *p*-phenylenediammonium dipicrate, 124043-03-4; **3d** *o*-phenylenediammonium dipicrate, 124043-04-5; **3e**, 124042-47-3; **4** potassium picrate, 124043-40-9; **5**, 15545-10-5; **6**, 124043-06-7; **7**, 124043-08-9; $Zn(OTf)_2$, 54010-75-2; *N*-(benzyloxycarbonyl)-L-histidine, 14997-58-1; 1-toxyl-5-chloro-3-oxapentane, 118715-74-5.